LETTERS

Ultraflat graphene

Chun Hung Lui[1], Li Liu[2], Kin Fai Mak[1], George W. Flynn[2] & Tony F. Heinz[1]

Graphene, a single atomic layer of carbon connected by sp^2 hybridized bonds, has attracted intense scientific interest since its recent discovery[1]. Much of the research on graphene has been directed towards exploration of its novel electronic properties, but the structural aspects of this model two-dimensional system are also of great interest and importance. In particular, microscopic corrugations have been observed on all suspended[2] and supported[3–8] graphene sheets studied so far. This rippling has been invoked to explain the thermodynamic stability of free-standing graphene sheets[9]. Many distinctive electronic[10–12] and chemical[13–15] properties of graphene have been attributed to the presence of ripples, which are also predicted to give rise to new physical phenomena[16–26] that would be absent in a planar two-dimensional material. Direct experimental study of such novel ripple physics has, however, been hindered by the lack of flat graphene layers. Here we demonstrate the fabrication of graphene monolayers that are flat down to the atomic level. These samples are produced by deposition on the atomically flat terraces of cleaved mica surfaces. The apparent height variation in the graphene layers observed by high-resolution atomic force microscopy (AFM) is less than 25 picometres, indicating the suppression of any existing intrinsic ripples in graphene. The availability of such ultraflat samples will permit rigorous testing of the impact of ripples on various physical and chemical properties of graphene.

The morphology of high-quality graphene crystals has been the subject of much attention. Detailed electron-diffraction studies of free-standing graphene monolayers[2] indicate the presence of an intrinsic rippling, with ~1-nm-high corrugations normal to the surface appearing over a characteristic lateral scale of 10–25 nm. It has been argued that these corrugations are necessary to stabilize the suspended graphene sheets against thermal instabilities present in ideal two-dimensional systems[9]. A comparable degree of height variation has also been reported in several studies of graphene monolayers deposited on insulating substrates[3–8]. This rippling has been invoked to explain many phenomena observed in graphene, such as the formation of electron–hole puddles[11,12], the suppression of weak localization[10], decreased carrier mobility[22] and enhanced chemical reactivity[13–15]. In addition, theoretical studies of graphene have predicted that graphene ripples will induce fascinating new phenomena, including the enhancement of spin–orbit coupling[16], the generation of an inhomogeneous density of states and the formation of zero-energy Landau levels in the absence of magnetic fields[17–20,23–25].

We report here the fabrication and characterization of high-quality ultraflat graphene monolayers by making use of a mica support that provides atomically flat terraces over large areas. Using high-resolution, non-contact mode atomic force microscopy (AFM) to characterize the morphology, we find that graphene on mica approaches the limit of atomic flatness. The apparent height variation of graphene on mica is found to be <25 pm over micrometre lateral length scales. This flatness, measured with a lateral spatial resolution of 7 nm, appears to be limited by instrument noise and is essentially identical (within 5 pm) to that observed for the surface of cleaved graphite crystals. Our results show that any intrinsic instability of graphene can be fully suppressed by deposition on an appropriate substrate. The availability of such a flat substance provides insight into questions of thermodynamic stability for this model two-dimensional system and also a reference material with which to determine the role of ripples in the panoply of observed and predicted phenomena.

The key to our experiments was the preparation of an atomically flat substrate for deposition of single-layer graphene crystals. For this purpose, we chose mica, a material composed of negatively charged aluminosilicate layers that are linked by single layers of potassium ions[27]. Since cleavage takes place readily along the potassium layer, atomically smooth surfaces with lateral dimensions as large as 100 μm can be routinely produced. Graphene monolayers were prepared by the standard method of mechanical exfoliation of kish graphite[1] on both mica and bulk SiO_2 substrates for comparative studies (see Methods).

We employed amplitude-modulation AFM in the non-contact mode to characterize the topography of the graphene samples. The AFM lateral and height resolution under scanning conditions were 7 nm and 23 pm, respectively. The AFM topographic images displayed in this paper are presented without filtering or smoothing. A third-order line and plane subtraction correction was applied to compensate for scanning drift and image bow. The roughness of the surface was characterized by the standard deviation σ of height distribution and the height correlation length l (see Supplementary Methods).

AFM topographic images acquired for regions surrounding the edges of graphene samples on both SiO_2 and mica substrates are shown in Fig. 1a, b. Histograms of the corresponding height distribution over the $200 \times 200\ nm^2$ regions of the surfaces are presented in Fig. 1c. For the bare SiO_2 surface, the parameters describing the height variation and correlation length (Table 1) are, respectively, $\sigma = 168$ pm and $l = 16$ nm. For the graphene monolayer on SiO_2, we find a comparable (or slightly diminished) degree of roughness, with $\sigma = 154$ pm and $l = 22$ nm, indicating that graphene monolayers largely follow the underlying substrate morphology.

In sharp contrast to these results, our AFM images on the mica substrate exhibit a much smoother landscape. For the bare mica surface, we obtain (see Table 1) $\sigma = 34.3$ pm and $l = 2$ nm. (As discussed below, we attribute the low value of l to residual AFM noise, rather than to physically meaningful features.) Taking the measured value of σ as a guide, the surface of mica is seen to be at least five times smoother than that of the SiO_2 substrate. When placed on such a flat mica terrace, graphene monolayers display an exceedingly flat structure, one quite different from that observed for graphene/SiO_2. This difference can be seen immediately by comparing the three-dimensional presentation of the AFM topographic images in Fig. 2a, b. More quantitatively, for graphene on mica, we obtain $\sigma = 24.1$ pm and $l = 2$ nm. This topography is at least five times smoother than that of graphene on SiO_2. Since the interlayer distance in bulk graphite is 340 pm, with an

[1]Departments of Physics and Electrical Engineering, Columbia University, 538 West 120th Street, [2]Department of Chemistry, Columbia University, 3000 Broadway, New York, New York 10027, USA.

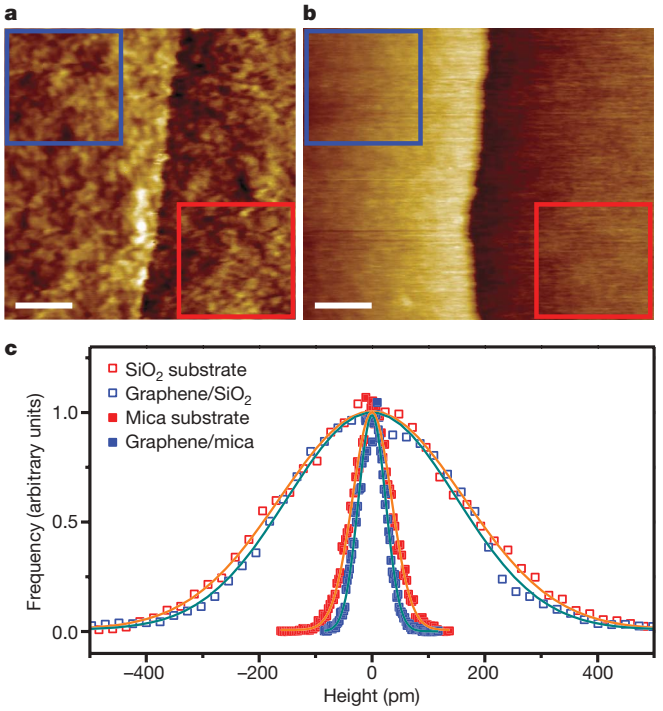

Figure 1 | AFM topographic images of different samples and the corresponding histograms of height. **a**, AFM image of a boundary between a graphene monolayer and a SiO_2 substrate. Graphene occupies the left-hand side of the image and the scale bar is 100 nm in length. **b**, As **a** for a graphene monolayer on a mica substrate. **c**, Height histograms for graphene on mica (solid blue squares), the mica substrate (solid red squares), graphene on SiO_2 (open blue squares), and the SiO_2 substrate (open red squares). The data, corresponding to the regions designated by the blue and red squares in the images of **a** and **b**, are described by Gaussian distributions (solid lines) with standard deviations σ of 24.1 pm, 34.3 pm, 154 pm, and 168 pm, respectively.

observed height variation of only 24.1 pm, we can consider graphene on mica as having reached the limit of atomic flatness with respect to ripples, that is, a height variation that is much less than the diameter of an atom when probed with our lateral resolution of 7 nm (see Supplementary Discussion).

Table 1 | σ and l of the images for different surfaces

	SiO_2	Graphene/SiO_2	Mica	Graphene/mica	Graphite
σ (pm)	168	154	34.3	24.1	22.6
l (nm)	16	22	2	2	2

The discussion of the flatness of the graphene/mica surface given above has been conservative in not attributing any of the observed height variation in the AFM images to instrumental noise. In fact, the results indicate that AFM noise is significant in measurements of flat surfaces. In particular, the correlation length of $l \approx 2$ nm calculated for the mica and the graphene/mica surfaces must arise largely from AFM noise, because any true physical features could only contribute to a correlation length comparable to or greater than the AFM spatial resolution of 7 nm. To address this issue, we made AFM measurements of the topography of cleaved kish graphite (Fig. 2c). The observed topography for the cleaved graphite surface is very similar to that of graphene/mica. Figure 2d compares the height histograms for graphite and graphene/mica. The widths of the distributions are, respectively, $\sigma = 22.6$ pm and $\sigma = 24.1$ pm. If we treat the graphite surface as entirely flat, then the measured standard deviation reflects the instrumental noise. Under the assumption that the instrumental noise adds in quadrature to any true height fluctuations, the values given above constrain the actual roughness of the graphene/mica sample to less than 8.5 pm.

Finally, in assessing the flatness of graphene, possible perturbations in its topography from tip-sample interactions must also be considered. To exclude the possibility that the observed flatness of graphene on mica might be produced through the suppression of ripples by the tip-sample interaction of the AFM probe, our AFM measurements have been carried out in a strictly non-contact mode, that is, one in which the tip/sample interaction was always attractive. Instead of pressing down on the surface at any time, the AFM tip is actually pulling slightly on the graphene sheet (see Supplementary Methods).

Since the discovery of intrinsic ripples in free-standing graphene, there has been considerable discussion of the role of substrate corrugation in determining the morphology of supported graphene

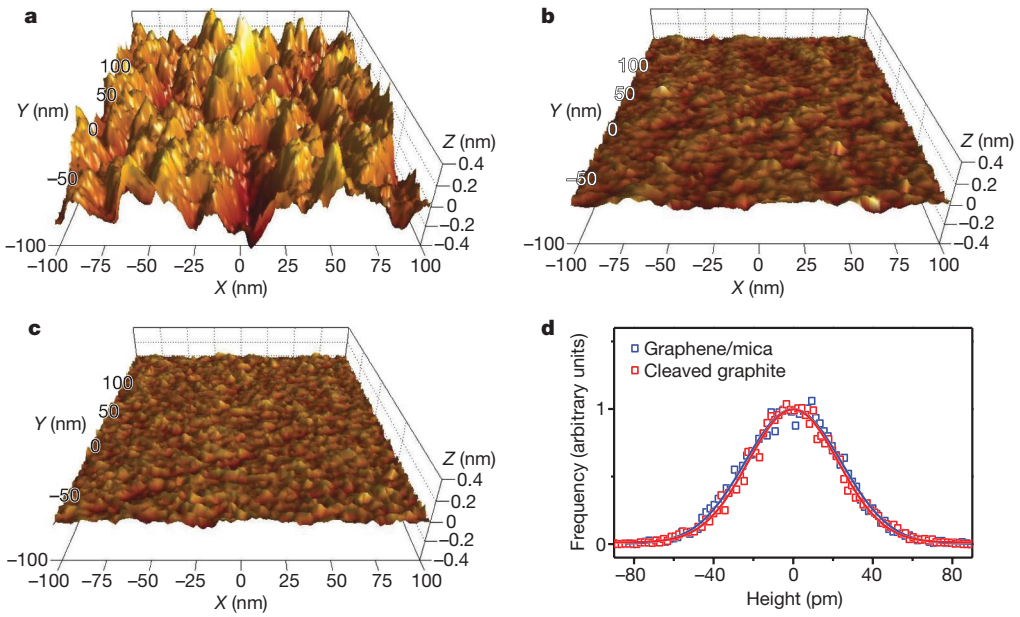

Figure 2 | Comparison of surface roughness for graphene on SiO_2 and on mica, and for cleaved graphite. **a**, **b**, Three-dimensional representations of the AFM topographic data for graphene on SiO_2 (**a**) and on mica (**b**) substrates. The images correspond to the regions in Fig. 1a and b designated by the blue squares. **c**, AFM image of the surface of a cleaved kish graphite sample. Images **a**, **b** and **c** correspond to 200 nm × 200 nm areas and are presented with the same height scale. **d**, Height histograms of the data in **b** as blue squares and in **c** as red squares. The histograms are described by Gaussian distributions (solid lines) with standard deviations σ of 24.1 pm and 22.6 pm, respectively.

monolayers[3–8]. Although the observed corrugation of supported graphene might well be an intrinsic feature[2,9] of the graphene monolayers in the experiments performed to date, a different explanation is equally possible. The roughness of the graphene surfaces may simply reflect the contours of the underlying substrates, which typically exhibit corrugation comparable to that observed in the supported graphene monolayers. Our measurements demonstrate unambiguously that intrinsic ripples in graphene, if they do exist, can be strongly suppressed by interfacial van der Waals interactions when this material is supported on an appropriate atomically flat substrate.

METHODS SUMMARY

Sample preparation. In our study we made use of grade V-1 muscovite mica substrates (15×15 mm^2, from Structure Probe) and produced graphene layers by the standard method of mechanical exfoliation of kish graphite[1]. Mica surfaces are known to be hydrophilic and readily adsorb water and carbon dioxide, as well as hydrocarbons. To minimize the presence of adsorbates at the graphene–mica interface, sample preparation was carried out in a glove box with water and oxygen concentrations below 1 p.p.m. (one part per million). For comparative studies, graphene monolayers were also prepared on bulk SiO_2 substrates. The SiO_2 substrates were carefully cleaned by sonication in methanol and the graphene samples were deposited by the same method of exfoliation of kish graphite, in this instance under ambient conditions. None of the samples described in this paper was subjected to any thermal processing.

Sample characterization. Graphene monolayers were identified on the mica substrate by optical microscopy, which was performed under ambient conditions. Although it is more difficult than for graphene samples deposited on an optimized SiO_2 overlayer on a silicon substrate, we were able to identify graphene monolayers directly by visual inspection. The modulation in reflectivity from a graphene monolayer still amounts to about 5% (Supplementary Fig. 1). Raman spectroscopy was applied for further characterization of the graphene samples[28] (Supplementary Fig. 2). From examination of the 2D mode Raman line, we confirmed the single-layer thickness of all the samples investigated in this paper. Also, the Raman spectra did not show any measurable D peak, indicating the high crystalline order of our samples. Our method of sample preparation was found to produce a significant yield of large graphene monolayers, with characteristic lateral dimensions ranging from tens of micrometres up to ~0.2 mm. The efficient deposition of large graphene single layers is attributed to the flat and clean surface of freshly cleaved mica.

Received 20 July 2007; accepted 1 October 2009.

1. Novoselov, K. S. *et al.* Two-dimensional atomic crystals. *Proc. Natl Acad. Sci. USA* **102,** 10451–10453 (2005).
2. Meyer, J. C. *et al.* The structure of suspended graphene sheets. *Nature* **446,** 60–63 (2007).
3. Stolyarova, E. *et al.* High-resolution scanning tunneling microscopy imaging of mesoscopic graphene sheets on an insulating surface. *Proc. Natl Acad. Sci. USA* **104,** 9209–9212 (2007).
4. Ishigami, M., Chen, J. H., Cullen, W. G., Fuhrer, M. S. & Williams, E. D. Atomic structure of graphene on SiO_2. *Nano Lett.* **7,** 1643–1648 (2007).
5. Booth, T. J. *et al.* Macroscopic graphene membranes and their extraordinary stiffness. *Nano Lett.* **8,** 2442–2446 (2008).
6. Knox, K. R. *et al.* Spectromicroscopy of single and multilayer graphene supported by a weakly interacting substrate. *Phys. Rev. B* **78,** 201408 (2008).
7. Stoberl, U., Wurstbauer, U., Wegscheider, W., Weiss, D. & Eroms, J. Morphology and flexibility of graphene and few-layer graphene on various substrates. *Appl. Phys. Lett.* **93,** 051906 (2008).
8. Geringer, V. *et al.* Intrinsic and extrinsic corrugation of monolayer graphene deposited on SiO_2. *Phys. Rev. Lett.* **102,** 076102 (2009).
9. Fasolino, A., Los, J. H. & Katsnelson, M. I. Intrinsic ripples in graphene. *Nature Mater.* **6,** 858–861 (2007).
10. Morozov, S. V. *et al.* Strong suppression of weak localization in graphene. *Phys. Rev. Lett.* **97,** 016801 (2006).
11. Martin, J. *et al.* Observation of electron-hole puddles in graphene using a scanning single-electron transistor. *Nature Phys.* **4,** 144–148 (2008).
12. Deshpande, A., Bao, W., Miao, F., Lau, C. N. & LeRoy, B. J. Spatially resolved spectroscopy of monolayer graphene on SiO_2. *Phys. Rev. B* **79,** 205411 (2009).
13. Liu, L. *et al.* Graphene oxidation: thickness-dependent etching and strong chemical doping. *Nano Lett.* **8,** 1965–1970 (2008).
14. Ryu, S. *et al.* Reversible basal plane hydrogenation of graphene. *Nano Lett.* **8,** 4597–4602 (2008).
15. Elias, D. C. *et al.* Control of graphene's properties by reversible hydrogenation: evidence for graphane. *Science* **323,** 610–613 (2009).
16. Huertas-Hernando, D., Guinea, F. & Brataas, A. Spin-orbit coupling in curved graphene, fullerenes, nanotubes, and nanotube caps. *Phys. Rev. B* **74,** 155426 (2006).
17. de Juan, F., Cortijo, A. & Vozmediano, M. A. H. Charge inhomogeneities due to smooth ripples in graphene sheets. *Phys. Rev. B* **76,** 165409 (2007).
18. Brey, L. & Palacios, J. J. Exchange-induced charge inhomogeneities in rippled neutral graphene. *Phys. Rev. B* **77,** 041403 (2008).
19. Guinea, F., Horovitz, B. & Le Doussal, P. Gauge field induced by ripples in graphene. *Phys. Rev. B* **77,** 205421 (2008).
20. Guinea, F., Katsnelson, M. I. & Vozmediano, M. A. H. Midgap states and charge inhomogeneities in corrugated graphene. *Phys. Rev. B* **77,** 075422 (2008).
21. Herbut, I. F., Juricic, V. & Vafek, O. Coulomb interaction, ripples, and the minimal conductivity of graphene. *Phys. Rev. Lett.* **100,** 046403 (2008).
22. Katsnelson, M. I. & Geim, A. K. Electron scattering on microscopic corrugations in graphene. *Phil. Trans. R. Soc. A* **366,** 195–204 (2008).
23. Kim, E. A. & Neto, A. H. C. Graphene as an electronic membrane. *Europhys. Lett.* **84,** 57007 (2008).
24. Vozmediano, M. A. H., de Juan, F. & Cortijo, A. Gauge fields and curvature in graphene. *J. Phys. Conf. Ser.* **129,** 012001 (2008).
25. Wehling, T. O., Balatsky, A. V., Tsvelik, A. M., Katsnelson, M. I. & Lichtenstein, A. I. Midgap states in corrugated graphene: ab initio calculations and effective field theory. *Europhys. Lett.* **84,** 17003 (2008).
26. Cortijo, A. & Vozmediano, M. A. H. Minimal conductivity of rippled graphene with topological disorder. *Phys. Rev. B* **79,** 184205 (2009).
27. Bragg, S. L. & Claringbull, G. F. *Crystal Structures of Minerals* Ch. 13 (G. Bell and Sons, 1965).
28. Ferrari, A. C. *et al.* Raman spectrum of graphene and graphene layers. *Phys. Rev. Lett.* **97,** 187401 (2006).

Supplementary Information is linked to the online version of the paper at www.nature.com/nature.

Acknowledgements We thank E. B. Newton and S. Li for their assistance in sample preparation and J. Shan, H. G. Yan and Z. Q. Li for discussions. This work was supported by grants from DARPA through the CERA programme (to T.F.H.), from the Nano Electronics Research Corporation (NERC) through the INDEX Center (to T.F.H.), and from the National Science Foundation (grant CHE-07-01483 to G.W.F.). Equipment and material support was provided by the US Department of Energy (grant DE-FG02-88-ER13937 to G.W.F.).

Author Contributions All of the authors contributed to the design of the experiment; C.H.L. and K.F.M. were responsible for the sample preparation, C.H.L. and L.L. characterized the samples by AFM imaging; C.H.L., L.L., and T.F.H. devised the method for and performed the data analysis; and C.H.L., G.W.F. and T.F.H. prepared the manuscript.

Author Information Reprints and permissions information is available at www.nature.com/reprints. Correspondence and requests for materials should be addressed to T.F.H. (tony.heinz@columbia.edu).

SUPPLEMENTARY INFORMATION

1. Supplementary Methods

Characterization of AFM resolution

We employed amplitude-modulation AFM in non-contact mode to characterize the topography of the graphene samples. The measurements were performed under ambient conditions using an ultrasharp AFM tip (DP14/Hi'Res-C/AIBS from MikroMasch) that consisted of a silicon cantilever with hydrophobic diamond-like spikes at the apex of a silicon tip. Typical values for the force constant, resonant frequency, and probe tip radius were, respectively, 5 N/m, 200 kHz, and 1 nm. The AFM lateral resolution was determined experimentally by characterizing the edges of graphene monolayers on the mica substrate. The height profile of the edge was fit by a step function convoluted with a Gaussian instrumental response function. We defined the AFM lateral resolution as the full width at half maximum (FWHM) of this response function. For the images presented in the paper, the instrumental resolution was found to be 7 nm. The height resolution was determined from residual noise in the AFM measurements. Using graphite surfaces as a reference, we found for our scanning conditions a root mean square height uncertainty of 23 pm.

Characterization of roughness of AFM topographic images

In our quantitative analysis of the images, we have consistently used areas of 200×200 nm^2 size. We characterized the roughness of AFM topographic images by constructing a histogram of the measured heights and calculating the standard deviation σ of this distribution. These histograms could be fit well by single Gaussian functions (for which the FWHM of the distribution is 2.36σ). Another useful description of the sample topography was given by the correlation length *l* of the height profile. This parameter, which defines the characteristic length of features observed in the AFM spatial images, is determined using the height correlation function

$$C(r) = \frac{1}{2\pi}\int h(x',y')h(x'+r\cos\theta, y'+r\sin\theta)dx'dy'd\theta$$

Where *h(x,y)* denotes the height of the AFM image at location *(x,y)*; and contributions

from different angles have been equally weighted. In evaluating this expression, we chose the scale of the height function $h(x,y)$ so that its mean value vanishes, in which case $\sigma=C(0)^{1/2}$. We then defined the correlation length l by requiring the correlation function to drop to e^{-1} of its peak value at a displacement of half of a correlation length, *i.e.,* $C(l/2) = e^{-1}C(0)$. Supplementary Fig. 3 shows the height correlation functions of both graphene on SiO_2 and graphene on mica.

Characterization of tip-sample interactions

To exclude possible perturbations in topography of the graphene layer from tip-sample interactions, we scanned our samples repeatedly under different conditions. Free amplitudes of the AFM cantilever from 30 nm down to 4.5 nm and amplitude set points ranging from 40% to 90% of the free amplitude were examined. No significant changes in the topography of graphene on mica were observed under any of these conditions. In all measurements, the phase shift between the driving force and the cantilever response was larger than 90°, indicating that the AFM is operating in the regime where the average tip-sample force is attractive [S1]. To treat these interactions in more detail, we examined the AFM tip motion on a graphite surface using the established VEDA simulation software [S2]. We found that the tip-sample force remains attractive for the full period of cantilever vibration whenever the cantilever free amplitude is less than 8 nm and the amplitude set point lies in the range from 40% to 90% of the free amplitude. Therefore, our AFM measurements in the lower range of cantilever amplitudes were carried out strictly in the attractive regime, and the possibility of tip-sample interactions leading to an artificially smoothed topography can be excluded.

2. Supplementary Discussion

Remarks on the topography of graphene on mica

We would like to make two observations about the topography of graphene monolayers on mica. First, although the graphene samples are very flat over areas on the sub-micron scale, variations in the topography can be seen when surveying the surface over distances of several microns. In particular, we have observed the presence of flat plateaus in the graphene topography, which rise abruptly by a height of ~0.4 nm above the lower

regions. We attribute these elevated regions to the formation of islands of molecular adlayers on the mica surface under the graphene sample. The precise nature and properties of these adlayer are under investigation. The presence of adsorbates may contribute to the observed slight local roughness. We find that σ varies from 20.8 to 24.1 pm for different regions of the graphene sample on mica. Second, given the limit of our AFM lateral resolution (7 nm), we cannot exclude the existence of sub-nanometre corrugation features (*e.g.*, atomic defects and vacancies) on the graphene surface. Based on modelling using the 7-nm AFM spatial resolution, the observed bound on the height variation of $\sigma < 25$ pm for graphene on mica allows us to exclude any periodic corrugations with a peak to trough separation greater than 5 nm (and an assumed amplitude of at least 100 pm). Further, isolated features of lateral extent greater than 1.5 nm (and a height of at least 100 pm) are also incompatible with our observed topography.

AFM images after Fourier filtering

Beyond the direct comparative study of topography of graphene/mica and the cleaved graphite surface, we also consider briefly the use of Fourier filtering to eliminate noise from the AFM images. Given the measured AFM lateral spatial resolution of 7 nm, we may safely remove any apparent spatial variation in the AFM images below this length scale without altering the actual physical content of the data. We carry out this procedure by applying a low-pass filter to the two-dimensional Fourier transform of the AFM topographic images. For our analysis, we apply a 6^{th}-order Butterworth low pass filter with a cutoff wavelength at 10 nm, which suppresses features in the images with a characteristic length scale below 5 nm. The suitability of this filtering procedure is confirmed by noting that it introduces only minimal broadening in the AFM image of the abrupt step at the graphene-mica edge. Using this low-pass filtering procedure for the graphite surface, we find that σ decreases significantly (from 22.6 pm to 12.4 pm). For graphene/SiO_2, on the other hand, σ drops only slightly (from 154 pm to 148 pm). This behavior is consistent with our expectation that AFM noise dominates on flat surfaces, but has relatively little effect for the more corrugated case of the SiO_2 substrate. For the sample of graphene/mica presented above, σ decreases from 24.1 pm to 16.1 pm. In some of the interior regions of the graphene/mica sample, σ is found after filtering to be as low as 11.4 pm.

3. Supplementary Figures

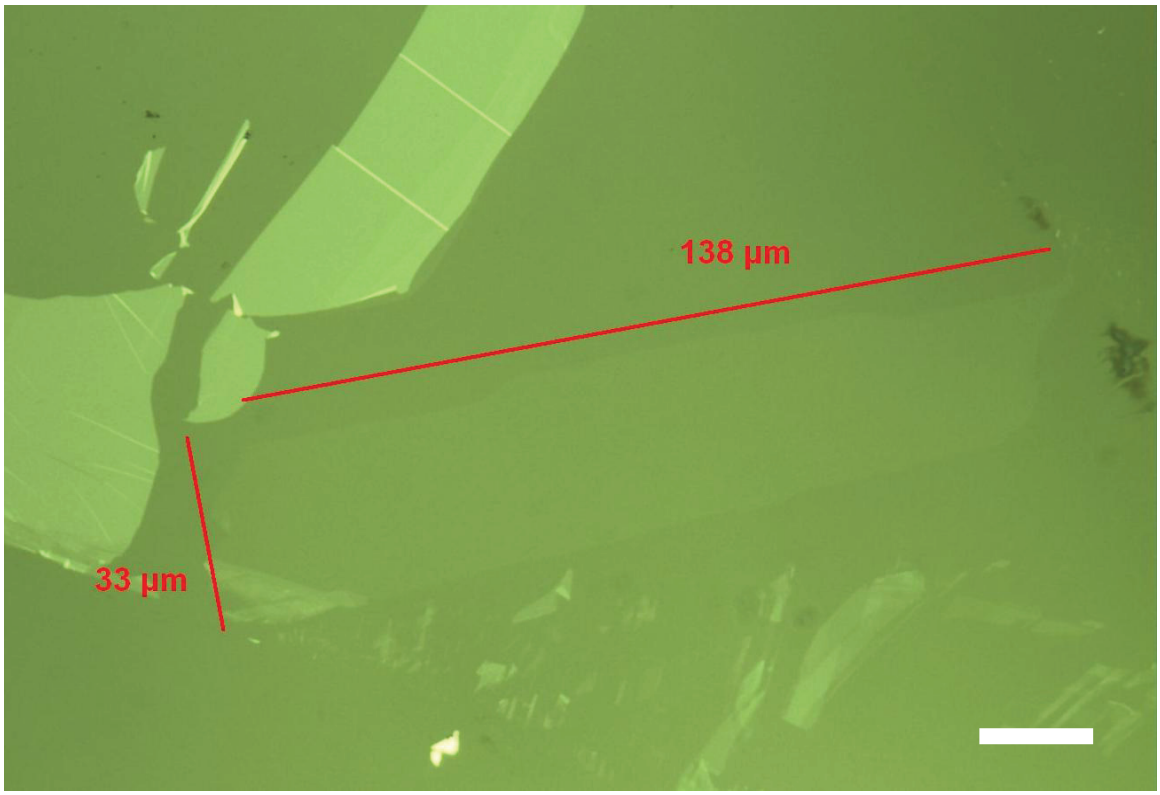

Figure S1. Image of a monolayer graphene sample on a mica substrate viewed by optical microscopy. The scale bar is 20 μm.

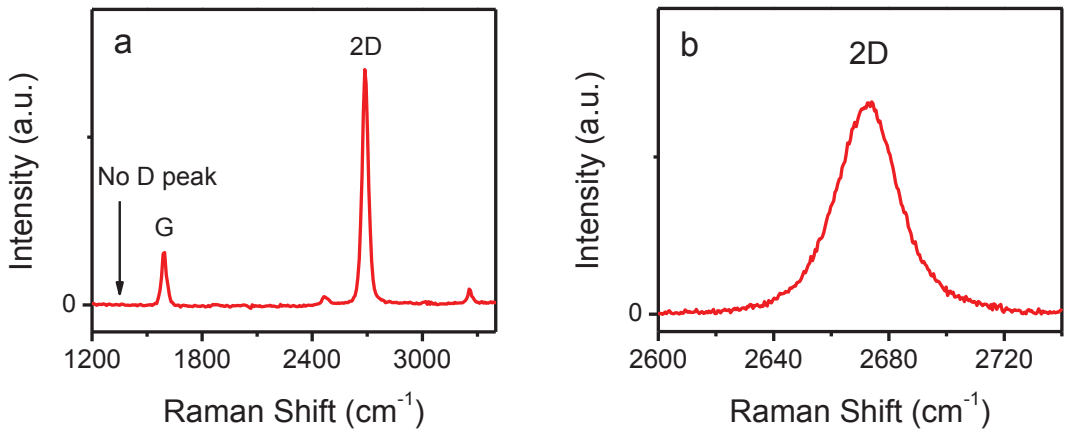

Figure S2. Raman spectra of the graphene monolayer in Figure S1 for an excitation wavelength of 532 nm. **a,** The Raman spectrum does not show any measurable D peak, indicating the high crystalline order of the sample. **b,** The 2D peak shows a narrow and symmetric profile, confirming that the sample is of monolayer thickness.

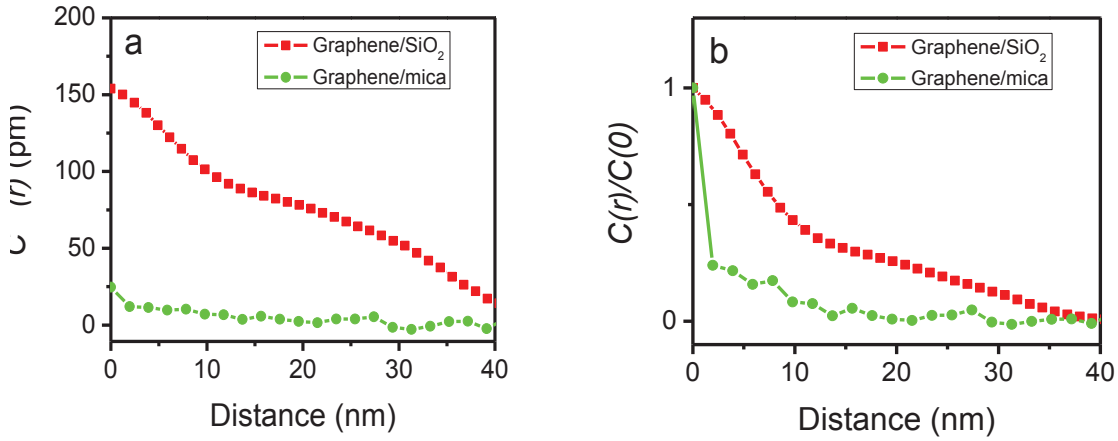

Figure S3. a, Square root of the height correlation function [$C^{1/2}(r)$]for graphene/SiO_2 and graphene/mica. **b,** Normalized height correlation function [$C(r)/C(0)$] for graphene/SiO_2 and graphene/mica.

Supplementary References:

[S1] Garcia, R. & San Paulo, A., Attractive and repulsive tip-sample interaction regimes in tapping-mode atomic force microscopy. *Phys. Rev. B* **60**, 4961-4967 (1999).

[S2] Melcher, J., Hu, S.Q., & Raman, A., Invited Article: VEDA: A web-based virtual environment for dynamic atomic force microscopy. *Rev. Sci. Instrum.* **79**, 061301 (2008).